Floating Electron States in Covalent Semiconductors

Yu-ichiro Matsushita, Shinnosuke Furuya, and Atsushi Oshiyama
Department of Applied Physics, The University of Tokyo, Tokyo 113-8656, Japan
(Received 17 November 2011; published 15 June 2012)

We report first-principles electronic-structure calculations that clarify the floating nature of electron states in covalent semiconductors. It is found that wave functions of several conduction- and valence-band states, including the conduction-band minima, do not distribute near atomic sites, as was taken for granted, but *float* in interstitial channels in most semiconductors. The directions and shapes of the interstitial channels depend on the crystal symmetry so that mysterious variation of the energy gaps in SiC polymorphs is naturally explained by considering the floating nature.

DOI: 10.1103/PhysRevLett.108.246404 PACS numbers: 71.20.Nr, 71.15.Mb, 71.20.Mq

Atoms comprise condensed matter in which electron states generally have their own atomic-orbital character and produce various physical and chemical properties. Some exceptions exist in spacious matter. Interlayer states in graphite [1] or intra- and intertube states in carbon nanotubes [2] are such examples, where the corresponding wave functions distribute *not* near atomic sites but in internal space, thus, *floating* in matter. These floating states are usually unoccupied but appear near Fermi levels or fundamental energy gaps and play crucial roles in excitation spectra [3,4] and ground-state properties [5], including occurrence of superconductivity [6,7].

It has been recognized that there is no room to allow such floating states in usual condensed matter. However, we here show by performing first-principles total-energy electronic-structure calculations that certain electron states of the conduction- and valence-bands in covalent semiconductors ranging from silicon to III–V compounds *float* in internal channels. Shapes of floating electron clouds depend on symmetry of the crystal and explain drastic and mysterious variation of the energy gaps in several polymorphs of compound semiconductors.

In sp^3-bonded covalent semiconductors, each atom is bonded with its four nearest neighbor atoms. The zinc blende and the diamond structures with cubic symmetry and the wurtzite structure with hexagonal symmetry are the typical two polymorphs, where the structural difference is only in the stacking of atomic planes along the axis of the inherent threefold rotational symmetry: The stacking sequences of ABC in the zinc blende and AB in the wurtzite structures, respectively. The stacking sequence is not limited to the above two cases. Hence, there are dozens of polymorphs labeled by the periodicity of the stacking sequence n and the symmetry (cubic or hexagonal) such as $2H$ (wurtzite), $3C$ (zinc blende), $4H$, and $6H$.

SiC indeed exhibits such polymorphs and the band gaps vary substantially, from 2.40 eV in $3C$ to 3.33 eV in $2H$ structures [8]. It is remarkable that the band gap varies by about 40% even though the local atomic structures are identical to each other. Such drastic variation has been discussed empirically in connection with the hexagonality [9] or in terms of wave scattering along the stacking direction [10], yet the underlying physics is still unclear.

Our calculations have been performed in the generalized gradient approximation (GGA) [11] in the density functional theory [12]. Norm-conserving pseudopotentials generated by using the Troullier-Martins scheme are adopted to describe the electron-ion interaction [13,14]. Valence-state Kohn-Sham (KS) orbitals and, thus, the valence electron density are expanded in terms of the plane-wave-basis set. The cutoff energy in the plane-wave-basis set is chosen to be 49 Ryd, except 46 Ryd for AlN and 81 Ryd for BN, to assure the accuracy in the total energy of 16 meV per molecular unit and 10 meV in the band gap. The $10 \times 10 \times 2$ k-point sampling in the hexagonal Brillouin zone (BZ) of $6H$ structure and equivalent densities in other structures are found to be enough to assure the same accuracy [15].

Figures 1(a)–1(c) show calculated energy bands of $2H$-SiC, $3C$-SiC, and $6H$-SiC (the stacking sequence is $ABCACB$). The conduction bands of the three polymorphs are qualitatively different in spite of the structural similarity: The conduction-band minimum is located at M point (equivalent to X point in the cubic BZ) in $3C$ and $6H$ structures, whereas it is at K point in the $2H$ structure. Furthermore, the lowest conduction band in the $3C$ structure is isolated and shift downwards substantially, making the band gap narrower by 0.7–0.9 eV than those in the $6H$ and $2H$ polymorphs [16].

Figure 1(d) shows the KS orbital at the conduction-band minimum (CBM) for $3C$-SiC. Surprisingly, the orbital distributes not near the atomic sites but floats in channels along $\langle 110 \rangle$ direction. The orbital changes its sign along the $\langle 110 \rangle$ channel with the periodicity of $\sqrt{2}a_0$ (a_0: lattice constant) and has nodes on the atomic plane containing Si atoms, thus avoiding atomic sites and distributing solely in the internal space. By examining the irreducible representation at M point, it is found that this phase variation of the Kohn-Sham orbital is allowed only at M point in the hexagonal BZ.

 © 2012 American Physical Society

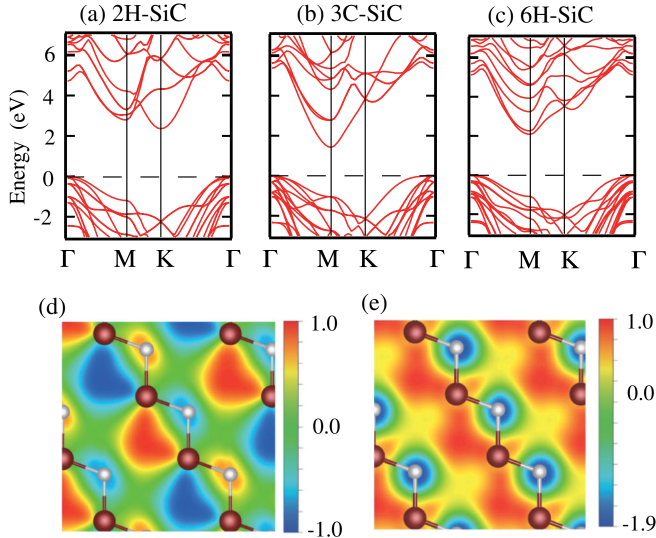

FIG. 1 (color online). Calculated energy bands [(a)–(c)] and wave functions (KS orbitals) [(d),(e)] of SiC. Energy bands for $2H$ (a), $3C$ (b), and 6 H (c) structures represented along symmetry lines in hexagonal BZ are shown. The energy of the valence-band top is set 0. Contour plots of the KS orbitals of the conduction band minimum at M (d) and of the fourth lowest conduction-band state at Γ (e) on $(0\bar{1}1)$ plane for $3C$-SiC. This M point corersponds to a point $X = (0, 0, 2\pi/a_0)$ in the cubic BZ. The value for each contour color is relative to the corresponding maximum absolute value. White and burgundy balls depict C and Si atoms, respectively.

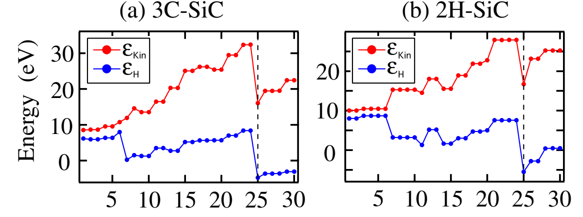

FIG. 2 (color online). Energy analyses of KS orbitals in SiC. The kinetic-energy contribution $\varepsilon_{\rm kin} = \langle\varphi_i| - \nabla^2/2|\varphi_i\rangle$ and the Hartree-energy contribution $\varepsilon_{\rm H} = \langle\varphi_i| \int \rho(\mathbf{r}')/|\mathbf{r} - \mathbf{r}'|d\mathbf{r}'|\varphi_i\rangle$ to the orbital energy of each KS state for M point in $3C$-SiC (a) and for K point in $2H$-SiC (b). The abscissa represents the ith KS state from the valence-band bottom and the 25th state is the conduction-band minimum.

Figure 2(a) shows the kinetic-energy and the Hartree-energy contributions to the orbital energy of each Kohn-Sham state at M point in $3C$-SiC. It is clear that the floating state gains the kinetic energy and the Hartree energy, compared with other states. The kinetic-energy gain obviously comes from the broad orbital distribution in the $\langle 110\rangle$ channel [Fig. 1(d)]. The Hartree-energy gain, on the other hand, comes from the ionic character of SiC. The electronegativity of C, 2.55, is larger than that of Si, 1.90, causing the electron transfer from Si to C in SiC. Our calculations indeed show that the electrostatic potential at the tetrahedral (T_d) interstitial site surrounded by 4 Si atoms is lower by 2.56 eV than that at another T_d site surrounded by 4 C atoms. The floating state has the maximum amplitude at the Si-surrounded T_d sites, thus floating in the $\langle 110\rangle$ channel. These energy gains cause the bandgap narrowing at M point.

The floating-state orbital with its sign unchanged along the $\langle 110\rangle$ channel is also possible. Such in-phase state is allowed, however, not at M point but at Γ point. Furthermore, the in-phase orbital inevitably has amplitudes at atomic sites, thus mixing with mainly s-character orbitals. We have indeed found such hybridized states at Γ point as shown in Fig. 1(e): The fourth lowest conduction-band at Γ which is the lowest conduction-band state at L point in the original cubic BZ is the antibonding state of the in-phase floating state and s orbitals of C. This mixing with atomic orbitals makes the resultant hybridized state shift upwards due to the kinetic- and Hartree-energy increase.

The CBM at K point is also of floating-state character. It extends along the $[1\bar{1}0]$, $[10\bar{1}]$, and $[01\bar{1}]$ channels on (111) plane and mixes with C atomic orbitals (Supplemental Material, Fig. 1 [18]). The kinetic-energy and the Hartree-enegy gains in the KS orbital energy for these floating states are 6.8 and 9.1 eV, respectively, compared with the valence-band top state, which is of usual atomic-orbital character.

The floating state at M point in $3C$-SiC distributes along the $\langle 110\rangle$ channel, which is slanted relative to [111] direction. A similar structural feature is observed in $6H$-SiC: There is a channel with the length of about $7a_0/2\sqrt{2}$ along $\langle\bar{2}201\rangle$, which is slanted relative to [0001] direction. We have indeed found that the Kohn-Sham orbital of the conduction-band minimum at M point in $6H$-SiC floats in this channel. Due to the limited length in the channel, the kinetic energy gain is smaller than in the $3C$ structure, and the energy gap in the $6H$ structure becomes wider [Fig. 1(c)].

In the $2H$ structure, such a slanted channel is absent. Instead, there are channels along $\langle 11\bar{2}0\rangle$ and $\langle 0001\rangle$ directions. We find that the CBM at K point in the $2H$ structure floats in the $\langle 11\bar{2}0\rangle$ channel (Fig. 3). This floating state distributes solely in the $\langle 11\bar{2}0\rangle$ channel with its phase changing consecutively by $\exp(i2\pi/3)$, thus avoiding the atomic sites on (0001) planes. It is also found that the floating state distributes closer to the planes of positively-charged Si atoms to gain the electrostatic energy. The phase change of the floating orbital along this channel is compatible with the symmetry of the Bloch state at K point. Analyses of the KS orbital energies shown in Fig. 2(b) clearly show that the energy gain comes from the kinetic- and the Hartree-energy parts.

The appearance of the conduction-band states which float in particular channels in SiC is a consequence of the existence of the internal space. It is noteworthy that the packing efficiency, p, of the sp^3-bonded structure is 0.34,

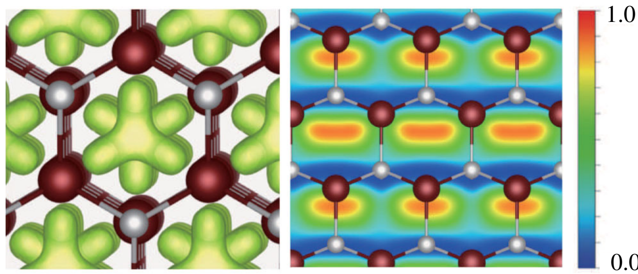

FIG. 3 (color online). KS orbital of the conduction-band minimum at K point of $2H$-SiC. Isovalue surface (left panel) and contour plot (right panel). The burgundy and the white balls depict Si and C atoms, respectively. In the left panel, the isovalue surface of the squared KS orbital viewed from [0001] direction is shown at its value of 80% of the maximum value. In the right panel, the contour plot of the squared KS orbital on $(1\bar{1}00)$ plane is shown.

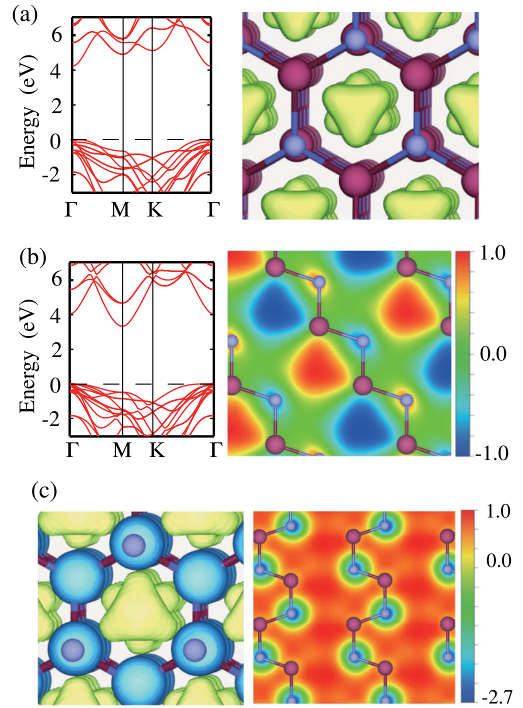

FIG. 4 (color online). Calculated energy bands and the conduction-band-minimum state of AlN in $2H$ and $3C$ structures. (a) Energy bands in a $2H$ structure and the isovalue surface of the squared KS orbital at K viewed from [0001] direction. The isovalue is taken as 80% of the maximum value. (b) Energy bands in a $3C$ structure and the contour plot of the KS orbital at M on $(0\bar{1}1)$ plane. (c) The isovalue surface (left panel) along [0001] direction and the contour plot (right panel) on $(11\bar{2}0)$ plane of the KS orbital at Γ in $2H$-AlN. In the left panel, the green surface corresponds to the value of 85% of the positive maximum value, whereas the blue surface corresponds to the negative value with the same absolute value. The value for each contour color in (b) and (c) is relative to the corresponding maximum absolute value. Burgundy and blue balls depict Al and N atoms, respectively.

which is extremely small compared with other crystal structures: $p = 0.52$ for simple cubic, $p = 0.68$ for body-centered cubic, $p = 0.74$ for face-centered cubic, and $p = 0.74$ for hexagonal close-packed structures, respectively. We then expect that the existence of the floating states is common to most covalent semiconductors. In addition, the difference in the electronegativity between the constituent atoms in SiC causes particular T_d interstitial sites to be energetically favorable.

We have therefore examined GaN, AlN, and BN. The calculated energy bands for these compounds clearly show the same feature as in SiC (Fig. 4 for AlN and Supplemental Material, Fig. 2 [18] for GaN and BN). We have found that the CBM at M point in $3C$ structure is the floating state in the slanted channel [Fig. 4(a)], whereas the CBM at K point in $2H$ structure is the floating state in the horizontal channel [Fig. 4(b)]. The cation tetrahedron surrounding the T_d interstitial site renders the M-point energy substantially low as in SiC. It is also found that the conduction-band minimum at Γ point has the floating character in AlN and GaN. The corresponding KS orbital distributes broadly around the T_d interstitial sites and the cation sites, exhibiting the floating character [Fig. 4(c)]. This characteristic is similar to the floating plus atomic-orbital state existing in the conduction bands at Γ point in SiC. Yet due to the ionicity in III-V compound semiconductors, the extension of the KS orbital to the cation sites makes the energy of the CBM state at Γ point lower. Owing to the competition with the electrostatic energy gain from the cation tetrahedron which makes the energy of the floating state at M-point low, the transition between the direct gap in the 2 H structure and the indirect gap in the $3C$ structure takes place for AlN (Fig. 4).

Even in elemental semiconductors the floating states exist, although they are not necessarily at the conduction-band minimum. We have examined cubic and hexagonal Si and C and indeed found the floating states. For $3C$-Si, Fig. 5(a) shows the KS orbital of the CBM state at M point (X point in cubic BZ). We have found this state has the bonding character of the floating and the atomic-orbital states. From the tight-binding picture, the CBM state at M point is the antibonding state of the s orbital and the neighboring p orbital, extending along ⟨001⟩ direction. This state is mixed with the floating state and thus the KS orbital distributes in the ⟨110⟩ channel. The KS orbital of the valence-band-bottom state at Γ is shown in Fig. 5(b). Basically, it is the bonding state of s orbitals, but it extends in the interstitial region substantially: The calculated amplitude at the interstitial T_d site is 23% of the maximum amplitude in sharp contrast with the valence-band-top state which is the bonding state of p orbitals with the amplitude at T_d site being about 1% of the maximum value. Hence the valence-band-bottom state is obviously the bonding state between s orbitals and the floating state. The KS orbital of

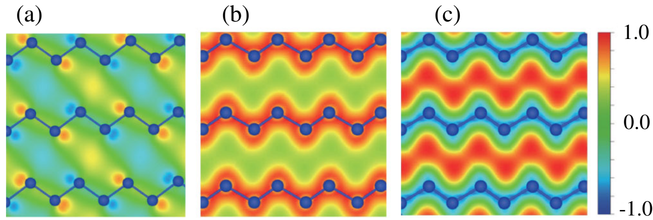

FIG. 5 (color online). Contour plots of the KS orbitals in 3*C*-Si. (a) Contour plot on (110) plane of the CBM state at *M*. The *sp* orbitals mixed with the floating state distributed in ⟨110⟩ channel. (b) Contour plot on (110) plane of the valence-band minimum state at Γ. The state is mainly of *s* bonding character but extends in the interstitial channel region. (c) Contour plot on (110) plane of the conduction-band state at Γ located at 7.81 eV above the valence-band top.

the antibonding counterpart which is located at 7.81 eV above the valence-band top, i.e., above the vacuum level, is shown in Fig. 5(c), clearly exhibiting the floating character.

Floating characters in the electron states are difficult to find in the linear combination of atomic orbitals basis sets. We have actually performed GGA calculations using the linear combination of atomic orbitals basis [19] for 2*H*- and 3*C*-SiC. The calculated Kohn-Sham orbitals lack the floating characters. Instead, they clearly show antibonding characters of the *s*- and *p*-orbitals (Supplemental Material, Figs. 3 and 4 [18]). This reflects the fact that linear combination of atomic orbitals basis sets are incomplete to describe the state distributing in the interstitial region unless additional orbitals are placed in the region far from atomic sites.

Total energies calculated in density-functional theory provide important information as to energetics. Table I shows calculated total energy difference among the polymorphs for SiC, GaN, AlN, BN, Si, and C including the polymorphs not observed yet. The total energy difference is in the range of 50 meV or less per molecular unit, indicating that the polymorphs in sp^3-bonded materials offer a good stage to examine characters of the floating states we have found.

In conclusion, our GGA calculations clarify that several conduction- and valence-band states do not distribute near atomic sites but float in the interstitial channels

TABLE I. Calculated total energies of 2*H*, 3*C*, and 6*H* structures for various sp^3-bonded semiconductors. The values are relative to the energy of the corresponding most stable structure in unit of meV per molecular unit. The 6*H* structures are not observed experimentally except for SiC, and the observed hexagonal structure of BN is planar.

	SiC	GaN	AlN	BN	Si	C
2*H*	7.1	0	0	35.5	22.3	50.9
3*C*	1.2	15.3	41.9	0	0	0
6*H*	0	9.5	28.4	9.6	4.0	12.8

in covalent semiconductors. It is found that the floating state is ubiquitous and stands alone in some cases and is mixed with atomic orbitals in others, affecting the energy bands substantially. These characteristics unrecognized in the past are related to the low packing efficiency in sp^3-bonded materials. The results are of scientific interest not only concerning the nature of electron states in condensed matter but also concerning the possibility of designing electronic properties by controlling the shapes of internal nanospace in matter.

We thank S. Hirota for discussions. This work was supported by the Grants-in-Aid for scientific research conducted by MEXT, Japan, under Contract No. 22104005. Computations were performed mainly at the Supercomputer Center in ISSP, The University of Tokyo.

[1] M. Posternak, A. Baldereschi, A. J. Freeman, E. Wimmer, and M. Weinert, Phys. Rev. Lett. **50**, 761 (1983).
[2] S. Okada, A. Oshiyama, and S. Saito, Phys. Rev. B **62**, 7634 (2000).
[3] M. Posternak, A. Baldereschi, A. J. Freeman, and E. Wimmer, Phys. Rev. Lett. **52**, 863 (1984).
[4] Th. Fauster, F. J. Himpsel, J. E. Fischer, and E. W. Plummer, Phys. Rev. Lett. **51**, 430 (1983).
[5] A. Oshiyama and S. Okada, in *The Oxford Handbook of Nanoscience and Technology*, edited by A. V. Narlikar and Y. Y. Fu (Oxford University, New York, 2010), Vol. II, p. 94.
[6] S. Saito and A. Oshiyama, Phys. Rev. Lett. **71**, 121 (1993).
[7] Y. Miyamoto, A. Rubio, X. Blase, M. L. Cohen, and S. G. Louie, Phys. Rev. Lett. **74**, 2993 (1995).
[8] For a review, *Properties of Silicon Carbide*, edited by G. L. Harris (INSPEC, London, 1995).
[9] W. J. Choyke, D. R. Hamilton, and L. Patrick, Phys. Rev. **133**, A1163 (1964).
[10] W. van Haeringen, P. A. Bobbert, and W. H. Backes, Phys. Status Solidi B **202**, 63 (1997).
[11] J. P. Perdew, K. Burke, and M. Ernzerhof, Phys. Rev. Lett. **77**, 3865 (1996).
[12] P. Hohenberg and W. Kohn, Phys. Rev. **136**, B864 (1964); W. Kohn and L. J. Sham, Phys. Rev. **140**, A1133 (1965).
[13] N. Troullier and J. L. Martins, Phys. Rev. B **43**, 1993 (1991).
[14] L. Kleinman and D. M. Bylander, Phys. Rev. Lett. **48**, 1425 (1982).
[15] The computation has been done with TAPP code: O. Sugino and A. Oshiyama, Phys. Rev. Lett. **68**, 1858 (1992); J. Yamauchi, M. Tsukada, S. Watanabe, and O. Sugino, Phys. Rev. B **54**, 5586 (1996); H. Kageshima and K. Shiraishi, Phys. Rev. B **56**, 14 985 (1997).
[16] Overall features of the calculated bands are in accord with the experiment, though the energy gaps are underestimated substantially as is characteristic of GGA. Yet, the relative difference in the energy gap among the polymorphs is well reproduced: In SiC, our GGA calculations provide the band gaps of 1.42, 2.08, and 2.36 eV for 3*C*, 6*H*, and 2*H* structures, whereas the corresponding

experimental values are 2.40, 3.10, and 3.33 eV, as reported in Ref. [8]. The quantitative description of the energy gaps, which is unnecessary in the present work, may be possible using the hybrid functional for the exchange-correlation energy [17].

[17] Y. I. Matsushita, K. Nakamura, and A. Oshiyama, Phys. Rev. B **84**, 075205 (2011).

[18] See Supplemental Material at http://link.aps.org/supplemental/10.1103/PhysRevLett.108.246404 for contour plots of the KS orbitals.

[19] The calculations have been done with the basis orbitals of *s* and *p* characters at each atomic site using OpenMX code: T. Ozaki, Phys. Rev. B **67**, 155108 (2003); T. Ozaki and H. Kino, Phys. Rev. B **69**, 195113 (2004).